EXCITED-STATE DYNAMICS OF BACTERIORHODOPSIN

TSUTOMU KOUYAMA, KAZUHIKO KINOSITA, JR., AND AKIRA IKEGAMI
The Institute of Physical and Chemical Research, Hirosawa 2-1, Wako-shi, Saitama 351, Japan

ABSTRACT Near infrared emission of bacteriorhodopsin at neutral pH and at room temperature was characterized by a large Stokes shift. This characteristic was lost in an acidic pH (~pH 2) where a remarkable enchancement (more than 10 times) in the fluorescence quantum yield accompanied the red shift in the main absorption band. It is suggested from fluorescence polarization measurements that the emission occurs from the first allowed excited state of the retinylidene chromophore, irrespective of pH. We suggest that the large Stokes shift observed at neutral pH is a result of a charge displacement (e.g., proton translocation) that occurs immediately after excitation, and is prevented by protonation (in the ground state) of an amino-acid residue in the protein.

INTRODUCTION

Bacteriorhodopsin, a single species of protein found in the purple membrane of *Halobacterium halobium*, has recently attracted many workers, primarily because of its important function as a light-driven proton pump. Bacteriorhodopsin contains a retinylidene chromophore, exhibiting a strong absorption band in the visible region. Light excitation of the chromophore in light-adapted bacteriorhodopsin (bR_{570}) initiates a photochemical reaction involving several photointermediates ($\rightarrow K_{590} \rightarrow L_{550} \rightarrow M_{412} \rightarrow O_{640} \rightarrow bR_{570}$), through which protons are actively translocated across the membrane (Stoeckenius et al., 1979; Ottolenghi, 1980). Recent studies using ultra-fast absorption spectroscopy have suggested another intermediate that appears ~1 ps after excitation and decays to K_{590} with a time constant of ~10 ps (Kaufmann et al., 1976; Applebury et al., 1978; Ippen et al., 1978). Characterization of this newly discovered intermediate, which is now called J_{625} (Ottolenghi, 1980), is important to better understand the energy conversion mechanism in bacteriorhodopsin, because it is believed that proton transfer and isomerization of the chromophore occur in the picosecond time scale (Lewis, 1978; Ottolenghi, 1980).

A basic question arises as to whether J_{625} belongs to the electronically excited or ground state. Fluorometry can be powerful in answering this question because bacteriorhodopsin exhibits a detectable emission in the red (or near-infrared) region (Lewis et al., 1976). A recent development of picosecond time-resolved fluorometry has allowed one to directly measure the fluorescence lifetime of the retinylidene chromophore (Alfano et al., 1976; Hirsch et al., 1976; Shapiro et al., 1978). Unfortunately, divergence of the values reported for the fluorescence lifetime (ranging from 1–14 ps) has left the discussions of the primary photoreaction confusing.

In the present work, we found that the quantum yield of the near-infrared emission was strongly dependent on the pH of the purple membrane suspension. More extensive investigations of the fluorescence intensity and polarization spectra under various experimental conditions provided important information about the excited-state dynamics of bacteriorhodopsin. Based on these investigations, we constructed a model of the primary photoreaction that can explain a large fraction of the recent data on bacteriorhodopsin.

MATERIALS AND METHODS

Sample Preparation

Purple membrane fragments of *Halobacterium halobium* were prepared according to the established procedure (Oesterhelt and Stoeckenius, 1974). A stacked sample of the purple membranes was obtained by drying the aqueous solution on a quartz plate in vaccuo (Henderson, 1975). By spraying a very dilute HCl solution on such a stacked sample and then drying again, another type of the stacked sample (exhibiting blue) was obtained. Sodium dodecyl sulfate (Bio Rad Laboratories, Tokyo, Japan), L1690 (lauryl ester of sucrose and 90% monoester; Ryoto Co., Tokyo, Japan), and glycerol (Merck Co., Inc., Tokyo, Japan) used in the present study were sufficiently nonfluorescent.

Fluorometry

Steady-excitation fluorometry was done with a photon-counting apparatus, in which red-sensitive photomultiplier tubes (model R943-02, Hamamatsu Corp., Shizuoka, Japan), were operated at −20°C (Kinosita et al., 1981).

Emission spectra were recorded using a 500 W high-pressure Hg lamp as an excitation light source; its emission line at 546 nm was selected by a series of optical filters (Koshin [Kanagawa, Japan] interference filter, Hoya C-500 and B-460 bandpass filters [Hoya, Tokyo, Japan] and $CuSO_4$ solution filter). Fluorescence emission from a thermostatically controlled sample was collected at a right angle to the excitation beam, and then passed through an analyzer (Karl Lambrecht, Tokyo, Japan), a light scrambler (depolarizer), an optical cut-off filter (Fuji-Film [Tokyo, Japan] SC-58 or -60), and an emission monochromator (Jobin Yvon; $\Delta\lambda$ = 4 nm). A corrected emission spectrum, S_{em}, (after excitation with unpolarized light) was computed as follows (Wahl, 1979):

$$S_{em}(\lambda) = [2I_v(\lambda) + I_h(\lambda) - 2I'_v(\lambda) - I'_h(\lambda)]/D_{em}(\lambda), \quad (1)$$

Address all reprint requests to A. Ikegami.

where I_v and I_h are two principal components of polarized fluorescence (vertical and horizontal) and $I'_{vh}(\lambda)$ are the Raman scattering components of the solvent. $D_{em}(\lambda)$ represents the wavelength dependence of sensitivity of the detection system, which was calculated using a standard tungsten lamp with a color temperature of 2,870 K.

Excitation spectra of the purple membrane suspensions were recorded using a 150-W Xenon lamp as a light source. A light beam from the lamp was passed through an excitation monochromator (Jobin Yvon; $\Delta\lambda$ = 4 nm), a Glan prism polarizer (Eiko Seiki Co., Tokyo, Japan), and a series of optical filters (a Hoya U-340 bandpass filter and Ni-, Co-, and Cu-SO_4 solution filters [between 270 and 330 nm] or a Hoya C-500 bandpass filter and $CuSO_4$ solution filters [between 330 and 680 nm]). The excitation light beam was then split into two beams by a half-mirror. One of them was directed into a quantum counter, in which an ethylene-glycol solution of rhodamine B (Wako Junyaku Co., Tokyo, Japan) (between 270 and 600 nm) or of methylene blue (Nakarai Co., Kyoto, Japan) (between 500 and 680 nm) was used as a fluorescent screen. The other beam was directed into a sample holder; fluorescence emission from a sample was passed through a series of cut-off filters (Hoya R-62 and Fuji-Film SC-74 or -82), by which a majority of light-scattering components (Rayleigh and Raman) were removed. The principal components of the polarized fluorescence, $I_{vv}(\lambda)$ and $I_{vh}(\lambda)$, were measured simultaneously with two photomultiplier tubes. Excitation spectra of total intensity $S_{ex}(\lambda)$ and anisotropy $r_{ex}(\lambda)$ were computed as follows:

$$S_{ex}(\lambda) = [I_{vv}(\lambda) + 2I_{vh}(\lambda) - I'_{v}v(\lambda) - 2I'_{vh}(\lambda)]/E(\lambda) \quad (2)$$

$$r(\lambda) = \frac{[I_{vv}(\lambda) - I_{vh}(\lambda) - I'_{vv}(\lambda) + I'_{vh}(\lambda)]}{[I_{vv}(\lambda) + 2I_{vh}(\lambda) - I'_{vv}(\lambda) - 2I'_{vh}(\lambda)]}, \quad (3)$$

where $I'(\lambda)$ are the Raman scattering components of the solvent; $E(\lambda)$ denotes the intensity of the excitation light beam, which was measured with the quantum counter.

Excitation polarization spectra of oriented purple membranes were also measured using the same fluorometer mentioned above, after the optical system had been altered. A stacked sample of the purple membrane was obliquely irradiated with an excitation light beam (making an angle of 42° with the plane of the sample), and the fluorescence emitted in a direction normal to the plate was collected. The following fluorescence polarizations (p^s and p^p) were recorded (see Appendix A for details):

$$p^s(\lambda) = [I_{vv}(\lambda) - I_{vh}(\lambda)]/[I_{vv}(\lambda) + I_{vh}(\lambda)] \quad (4)$$

$$p^p(\lambda) = [I_{hv}(\lambda) - I_{hh}(\lambda)]/[I_{hv}(\lambda) + I_{hh}(\lambda)], \quad (5)$$

where the first and second suffixes of I denote the directions (vertical or horizontal) of polarization plane of the excitation light and of the emission light, respectively (both the excitation and emission beams were propagating in a horizontal plane).

The fluorescence quantum yield measurements were done according to the method originally developed by Weber and Teale (1957) and then improved by Eastman (1967). A dilute solution of Ludox (DuPont Co., Ltd., Wilmington, DE) was used as a standard light scatterer. By using this method, the fluorescence quantum yields of quinine sulfate in 0.1 N H_2SO_4, and of tryptophan in water were determined to be 0.53 and 0.18, respectively; both of these values agree with those used in most of the previous papers.

RESULTS

Near-Infrared Emission of Bacteriorhodopsin at Neutral pH

Fluorescence emission spectra of light-adapted bacteriorhodopsin were recorded at room temperature, using an emission line at 546 nm from a 500-W Hg lamp as an excitation light source. The closed circles in Fig. 1 show the spectrum observed for the purple membrane suspension at pH 7.0 (10 mM PO_4). Owing to a high detection sensitivity (even for near-infrared light) of the present fluorometer, it was possible to extend the recording region up to 900 nm. The broken line in Fig. 1 shows the wavelength dependence of the detection sensitivity.

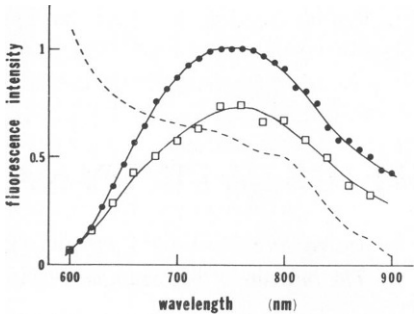

FIGURE 1 Corrected emission spectra of fluorescence from the light-adapted (●) and dark-adapted (□) purple membranes suspended at pH 7.0. A dilute suspension of purple membranes (0.15 mg protein/ml) was excited at 546 nm. The broken line shows the wavelength dependence of detection sensitivity of the present fluorometer.

The emission spectrum of dark-adapted bacteriorhodopsin was also determined. Because a direct recording of its emission spectrum was difficult (because the excitation light beam needed for this purpose was too intense), the following method was used. First, a purple membrane suspension was irradiated by an excitation beam (from a 150-W Xe-lamp) that was weak enough to keep bacteriorhodopsin in the dark-adapted state, and the fluorescence emission was viewed only through an optical cut-off filter that removed the majority of the light-scattering components (including Raman components of the solvent). With this optical system, the change of the fluorescence intensity (above 740 nm) during the dark adaptation was followed. When the excitation wavelength was set at 525 nm, where the absorption coefficient of bacteriorhodopsin did not change with its dark-light adaptation reaction, the fluorescence intensity observed for dark-adapted bacteriorhodopsin was 0.74 times as strong as that observed for light-adapted bacteriorhodopsin. Then, the purple membrane suspension was irradiated by an intense excitation beam, and the fluorescence was viewed with two detection systems simultaneously. One of them, the same system as was just mentioned above, was used to monitor how much the excitation beam shifted the equilibrium between the dark- and light-adapted states; the other system was equipped with an emission monochromator. The outputs of these two systems were recorded while the sample was gradually light adapted by the excitation beam, and the fluorescence intensity of dark-adapted bacteriorhodopsin (relative to that of the light-adapted one) was calculated at each emission wavelength. The result is shown by the open

squares in Fig. 1. This emission spectrum basically has the same features as that of light-adapted bacteriorhodopsin, except for the absolute fluorescence intensity.

The fluorescence quantum yield of light-adapted bacteriorhodopsin was determined to be 2.5×10^{-4}, using the method shown in Materials and Methods. From this result and the data shown in Fig. 1, the fluorescence quantum yield of dark-adapted bacteriorhodopsin was estimated to be $\sim 1.8 \times 10^{-4}$. It has been reported that the dark-adapted purple membrane contains an equimolar mixture of two retinal isomers (13-*cis* and all-*trans* retinal), whereas the light-adapted one contains more than 90% of all-*trans* retinal (Oesterhelt et al., 1973; Sperling et al., 1977; Mowery et al., 1979). Thus the fluorescence quantum yields of 13-*cis* and all-*trans* retinal isomers in bacteriorhodopsin are $0.7–1.2 \times 10^{-4}$ and $2.5–2.7 \times 10^{-4}$, respectively, if the *trans* component in dark-adapted bacteriorhodopsin has the same emission as in light-adapted bacteriorhodopsin.

The fluorescence intensity of dark-adapted bacteriorhodopsin was almost insensitive to temperatures >0°C (open circles in Fig. 7).

Near-Infrared Emission of Bacteriorhodopsin at Acidic pH

The efficiency of emission increases considerably at acidic pH. In Fig. 2 *c*, the fluorescence intensity observed above 740 nm after excitation at 540 nm (divided by the protein concentration) is plotted as a function of pH. This pH titration curve was obtained by adding HCl (or NaOH) to the dark-adapted purple membrane suspension ($OD_{560} \sim 0.04$) containing 1 mM phosphate buffer (20°C). Under these conditions, the most intense emission occurred around pH 1.7, where the fluorescence intensity was ~15 times stronger than at neutral pH and the absorbance was smallest. Such a large enhancement in the fluorescence intensity at acidic pH was also observed in the presence of 67% glycerol, in which aggregation of the purple membranes was diminished. A similar result was obtained even when bacteriorhodopsin existed as a monomer in a solution containing 10 mM L1690 (lauryl ester of sucrose and 90% monoester) (Naito et al., 1981). At higher acidity, the fluorescence intensity decreased again. In contrast to the dramatic change in the acidic pH region, only a small change was observed in the alkaline pH region.

The pH dependence of the fluorescence intensity correlated strongly with the change in the absorption spectrum. Fig. 2 *a* shows the pH titration curve of the difference absorbance (OD_{565}–OD_{630}) observed under the same solvent condition (except for the protein concentration). The two pH titration curves (Figs. 2 *a* and *c*) show similar profiles, except for the inversion, in the acidic pH region. In addition, both of these titration curves were strongly affected by the composition of the solvent. A large

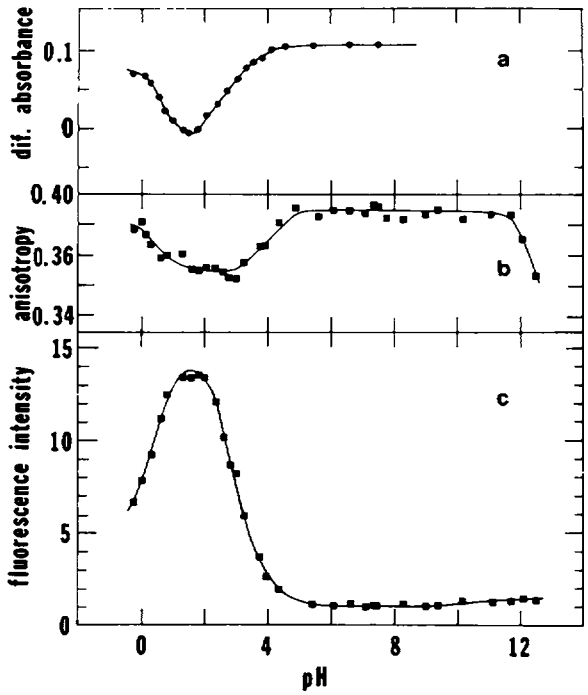

FIGURE 2 pH titration of the fluorescence intensity shown in *c* and anisotropy shown in *b* of the purple membrane. The purple membrane suspension (0.06 mg protein/ml) containing 1 mM PO_4 (at 20°C) was excited at 540 nm and fluorescence emission above 740 nm was collected. *a* shows the difference (*dif.*) absorbance (OD_{565}–OD_{630}).

enhancement in the fluorescence intensity was also observed when a very low concentration (0.01%) of sodium dodecyl sulfate (pH 4.0) was added, which was accompanied by a red shift of the absorption peak to 600 nm. On the contrary, in the presence of a higher concentration of salt (10 mM phosphate buffer), the pH at which the fluorescence intensity became the most intense was shifted towards a lower pH (pH 1.4). A similar effect of ionic strength has been observed in the pH titration of the absorption spectrum of bacteriorhodopsin (Fischer and Oesterhelt, 1979). As investigated, the large enhancement in the fluorescence intensity was always accompanied by the red shift of the absorption peak (from 560 to 605–610 nm). (Another example was obtained when the purple membrane suspension was deionized.) According to Mowery et al. (1979), the red shift of the absorption peak of bacteriorhodopsin is caused by the formation of the acidic form bR_{605}^{acid}, which is replaced with another acidic form bR_{565}^{acid} in a highly acidic pH region. The present result indicates that the acidic form bR_{605}^{acid} exhibits a much higher fluorescence quantum yield than the other forms.

Bacteriorhodopsin emission at the acidic pH region was characterized by a small Stokes shift, compared with that observed at neutral pH. A typical example of pH dependence of the emission spectrum of bacteriorhodopsin is shown in Fig. 3, where the spectra are normalized to have the same intensity at peak. Although the wavelength of the

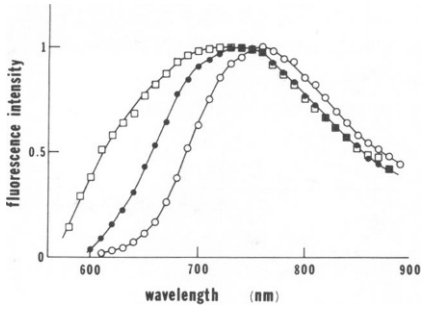

FIGURE 3 Corrected fluorescence emission spectra of the purple membrane suspended at pH 2.6 (○), pH 0.2 (●), and pH −0.5 (□). Excitation wavelength was 546 nm. 67% Glycerol and various concentrations of HCl were used as solvents at 20°C.

absorption peak was shifted from 560 to 605 nm when the pH was lowered from neutral to 2.6, the wavelength of the emission peak (750 nm) scarcely changed (the emission bandwidth itself became narrow; see open circles in Fig. 3 compared with closed circles in Fig. 1). Further lowering the pH, however, was accompanied by a large blue shift in the emission spectrum as well as the blue shift in the absorption spectrum.

The fluorescence anisotropy was found to change when the pH was lowered. The very high value [r (>740 nm) = 0.394 ± 0.003] observed at neutral pH was replaced with a lower value [r (>740 nm) = 0.36 ± 0.01] whenever the color of the purple membrane suspension turned to blue. Fig. 2 *b* shows the pH titration curve of the fluorescence anisotropy that was obtained at the same time as the curve shown in Fig. 2 *c*. In these figures the fluorescence anisotropy has considerably decreased at pH 4.0, where the fluorescence intensity is only twice as strong as that at neutral pH; the low constant value for anisotropy is seen over a wide pH region (between 1.0 and 4.0).

Excitation Spectra of the Purple Membrane Suspension

Information concerning the electronic structure of the retinylidene chromophore in bacteriorhodopsin was obtained from the excitation polarization spectra of the purple membrane suspensions. In Fig. 4, the fluorescence anisotropy in *a* and total intensity in *b* that were observed above 740 nm (or 820 nm) upon excitation of a dilute suspension of the dark-adapted purple membrane (OD_{560} or $OD_{600} \cong 0.02$) are plotted as a function of excitation wavelength (Eq. 3). The closed circles and open squares in the figure represent the data obtained at neutral pH (10 mM phosphate) and at an acidic pH (pH 4.0; 10 mM acetate buffer and 0.02% sodium dodecyl sulfate), respectively. (Replacement of the latter solvent by 67% glycerol (pH 2.6) essentially did not alter the result.) It can be seen from the excitation anisotropy spectra that three different electronic-transition bands appear in the wavelength region above 300 nm, irrespective of pH. That is, a main band with an apparent peak at 565 nm (or 605 nm at the acidic pH), a weak band ~400 nm (or 420 nm), and a very weak band just above 300 nm. (Let these three bands be called α, β_1, and β_2 bands, respectively.) There is no indication that another weak band exists in the red side of the main band; every excitation anisotropy spectrum showed a constant value over the corresponding wavelength region. The slope from 320 to 370 nm in the excitation anisotropy spectrum suggests that the β_2 band extends to 360 nm. It is unlikely that the β_2 band comes from an aromatic residue in the protein. (Note that the circular dichroism spectrum of the purple membrane suspension has a negative peak at ~320 nm.) Thus the above result suggests that the retinylidene chromophore has three absorption bands above 300 nm. This seems valid for both the two retinal isomers in dark-adapted bacteriorhodopsin, because the light adapation (at neutral pH) is accompanied by only a slight change in the absorption spectrum between 300 and 470 nm (a slight increase between 370 and 440 nm and a slight decrease between 300 and 350 nm).

The excitation intensity spectra (Fig. 4 *b*) gave information about the excitation-wavelength dependence of the fluorescence quantum yield. The absorption spectra of the purple membrane suspension at pH 7.0 and at pH 4.0 (in the presence of 0.02% sodium dodecyl sulfate) are shown in Fig. 4 *c*, where the broken line represents the contribution from the turbidity of the purple membrane suspension (this line was calculated as shown in a previous paper; Kouyama et al., 1981). At neutral pH, the excitation intensity spectrum can be superimposed considerably well on the absorption spectrum (after correction for the turbidity). Small discrepancies between these two spectra result because the dark-adapted purple membrane contains two kinds of retinal isomers, whose fluorescence quantum yields are different from each other. It is thus suggested that the fluorescence quantum yield of the retinylidene chromophore is almost independent of the excitation wavelength. On the contrary, at the acidic pH, large discrepancies were observed between the excitation and absorption spectra; e.g., note the position of the peak of the α band or the relative amplitude of the $\beta_{1,2}$ bands with reference to the α band. It is unlikely that possible aggregation of the membranes caused a large distortion in the absorption spectrum, because a similar result was obtained for the bacteriorhodopsin monomer in 10 mM L1690 solution. Some parts of the discrepancies (e.g., around the main band) appear to be caused by an equilibrium between the acidic form bR_{605}^{acid} with a high fluorescence quantum yield and the other forms with low fluorescence quantum yields. It seems probable that the membrane containing only the acidic form bR_{605}^{acid} would have an absorption peak at 610 nm. However, to explain the excitation spectra over the entire wavelength region, we needed to consider the possibility of variation in the fluorescence quantum yield with excitation wavelength. It appears that the excitation of β_1

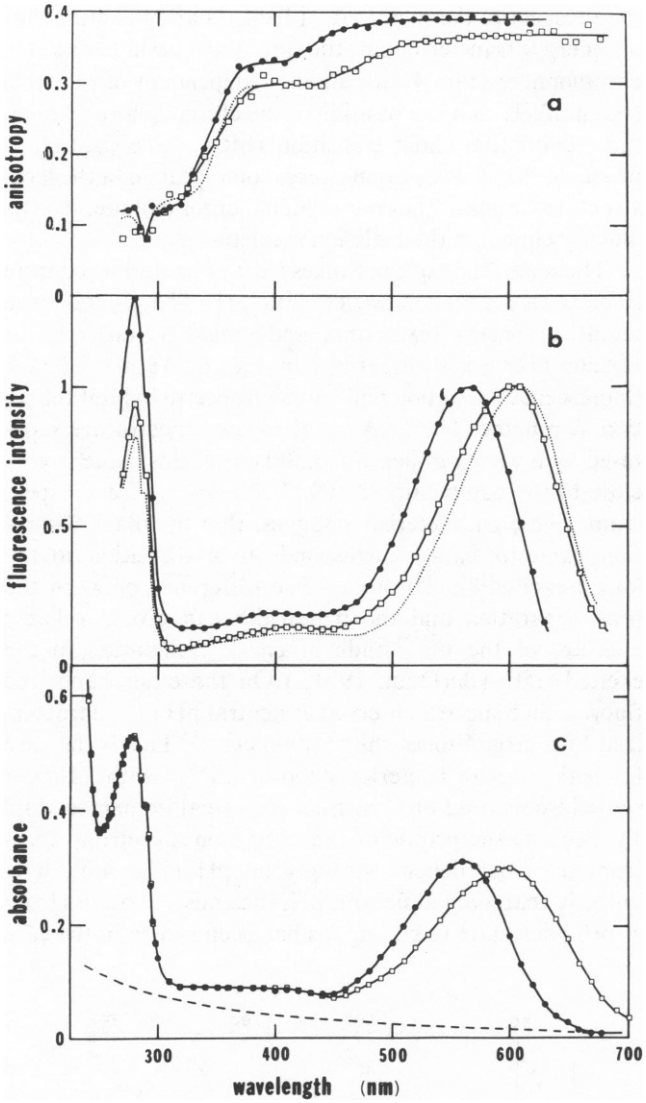

FIGURE 4 Excitation spectra of the total fluorescence intensity are shown in *b* and anisotropy are shown in *a* of the purple membrane suspensions. Fluorescence emission was collected above 740 nm. The solvent conditions were (at 20°C) 10 mM phosphate buffer, pH 7.0 (●); 0.02% sodium dodecyl sulfate and 10 mM acetate buffer, pH 4.0 (□); and 67% glycerol at pH 2.6 (dots). *c* shows absorption spectra observed under the corresponding solvent conditions.

or β_2 causes a smaller fluorescence quantum yield than the excitation of the α band. (Because the two spectra in Fig. 4 *c* can be superimposed on each other in the wavelength region between 270 and 450 nm, it may be that the efficiency of energy transfer from the aromatic residues to the retinylidene chromophore does not change much with pH.)

Fluorescene Polarization of the Oriented Purple Membrane

Information concerning the orientation of the absorption dipole moments of the chromophore was obtained by investigating the polarization degrees of fluorescence from the oriented purple membrane. A stacked sample of the purple membranes on a quartz plate was obliquely irradiated by linearly polarized light, and polarized fluorescence was viewed from the direction normal to the plate (Fig. 10). Depending on whether the polarization plane of the incident beam is perpendicular or parallel to the plane of incidence, two kinds of fluorescence polarization degrees, p^s and p^p, are defined (see Fig. 10 and Appendix A for details). In Fig. 5, the polarization degrees p^s (open circles) and $|p^p|$ (closed circles, the values were negative), are plotted as a function of excitation wavelength; the upper and lower panels show the data obtained for the sample exhibiting purple (neutral pH) and for the sample exhibiting blue (acidic pH), respectively.

These spectra (as well as the data in Fig. 4 *b*) were analyzed by using Eqs. A7 and A9. The result of analysis is shown in Table I, where γ denotes the angle between the directions of the absorption and emission dipole moments and $\Delta\phi$ represents its component within the plane of the membrane. Because some of the assumptions used to derive Eqs. A7 and A9 may not reflect the actual system, the physical meaning of each angle appearing in Table I must be carefully interpreted (see Eqs. A10–A13); e.g., in the case that reorientation of the emission dipole moment occurs during the excited state, the figures about γ and $\Delta\phi$ are only time averages of the corresponding quantities.

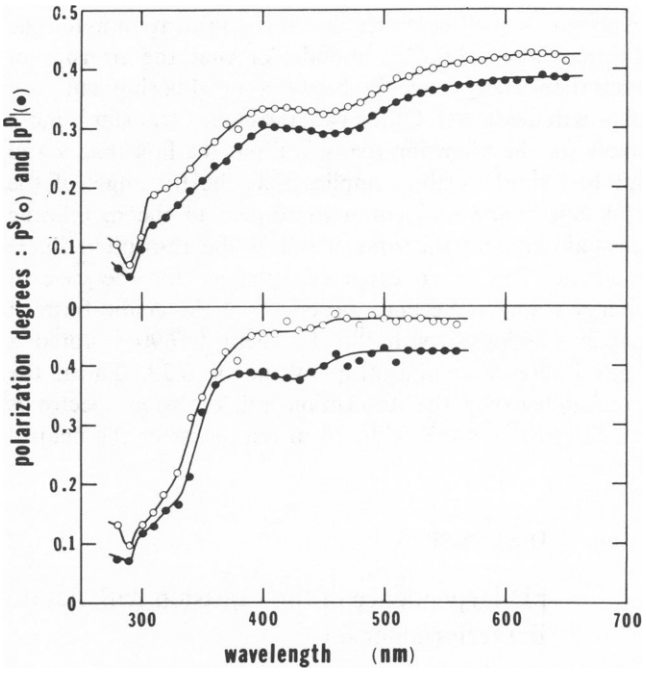

FIGURE 5 Excitation spectra of the polarization degrees p^s(○) and $|p^p|$ (●) of fluorescence from oriented purple membranes. Values of p^p are negative over the entire region. A plate with a stacked sample of the purple membranes was obliquely irradiated with an excitation beam and fluorescence emission above 740 nm was collected in a direction normal to the plate. The data shown in the lower and upper panels were obtained for the stacked samples exhibiting purple (at neutral pH) and blue (at an acidic pH), respectively.

TABLE I
ORIENTATIONAL CORRELATION BETWEEN THE ABSORPTION AND EMISSION DIPOLE MOMENTS OF THE RETINYLIDENE CHROMOPHORE IN THE PURPLE MEMBRANE

pH	Band	λ	r	p^s	$-p^p$	γ	Δφ	θ_{ex}
		nm					*degree*	
Neutral	α	560	0.394	0.480	0.425	7*	8*	70
	β_1	410	0.328	0.458	0.375	20	12	65
	β_2	310	0.12	0.20	0.13	43	33	54
	L_b	290	0.08	0.10	0.07	47	39	57
Acid	α	610	0.368	0.428	0.388	13*	14*	72
	β_1	440	0.298	0.333	0.298	24	23	71
	β_2	310	0.12	0.19	0.14	43	33	59
	L_b	290	0.08	0.07	0.05	47	41	57

Here γ is the angle between the directions of the absorption and emission dipole moments, whose value was calculated from the fluorescence anisotropy (Fig. 4) using the formula: $r = 2/5\ (3/2\cos^2\gamma - 1/2)$. There is the following relationship: $\cos\gamma = \cos\theta_{ex}\cos\theta_{em} - \sin\theta_{ex}\sin\theta_{em}\cos\Delta\phi$, where the angles θ_{ex} θ_{em} and Δφ are defined in Fig. 10. The values of θ_{ex} and Δφ were calculated using Eqs. A7 and A8.

*These values may be considerably overestimated because fluorescence depolarization effects due to the light scattering and interference within the samples were not taken into account.

For the α band, the angle γ, between the absorption and emission dipole moments is significantly larger in the acidic form than in the membrane at neutral pH. Simple explanations will be either that the acidification made the chromophore somewhat mobile, or that the transfer of excitation energy occurs between neighboring chromophores at acidic pH. Of the two, the energy transfer is more likely for the following reasons. First, the fact that γ and Δφ had similar values implies that the tilt angle of the emission dipole moment with respect to the membrane normal remained the same as that of the absorption dipole moment. This is an expected behavior for the case of energy transfer. Second, dispersion of the acidic form of bacteriorhodopsin with the detergent L1690 restored a high fluorescence anisotropy value of 0.39. Third, the overlap between the absorption and emission spectra is much larger for the acidic form than it is for the neutral form.

DISCUSSION

pH Dependence of the Emission Kinetics of Bacteriorhodopsin

We found that acidification of the purple membrane suspension causes a remarkable enhancement (>10 times) in the fluorescence quantum yield (Fig. 2). The fluorescence enhancement always accompanied the red shift in the main absorption band. This phenomenon was also observed for the bacteriorhodopsin monomer in 10 mM L1690 solution. However, the tilt angle of the chromophore with respect to the membrane (Table I) and the efficiency of energy transfer from the aromatic residues to the chromophore (Fig. 4) are almost independent of pH. It is thus unlikely that the position of the chromophore changes much with the acidic transition ($bR_{560} \rightarrow bR_{605}^{acid}$). It is probable that acidification causes some change in the local structure around the retinylidene chromophore, consequently changing the emission mechanism.

The magnitude of the Stokes shift of bacteriorhodopsin fluorescence emission varies with pH. The fluorescence intensity spectra (excitation and emission) observed at various pHs are summarized in Fig. 6. At pH 2.6, the fluorescence excitation and emission spectra exhibit reflection symmetry. The peaks of these two spectra are separated by a wavenumber of ~3,500 cm^{-1}; this value is very close to the bandwidth (3,100–3,300 cm^{-1}) of each spectrum. These characteristics suggest that the main absorption band (α band) corresponds to a transition to the lowest-excited singlet state. (The difference between the peak separation and the bandwidth can give a reliable measure of the magnitude of energy relaxation in the excited state [Berlman, 1971].) On the other hand, the fluorescence spectra observed at neutral pH are characterized by a large Stokes shift (5,000 cm^{-1}). This is the case for both types of bacteriorhodopsin (bR^{trans} with all-*trans* retinal isomer and bR^{cis} with 13-*cis* retinal isomer; see Fig. 1). Because the profile of the excitation anisotropy spectrum does not depend strongly on pH (Fig. 4 *a*), it is unlikely that, only at neutral pH, the emission occurs from a forbidden state (e.g., $^1A_g^-$, as has been shown in the case

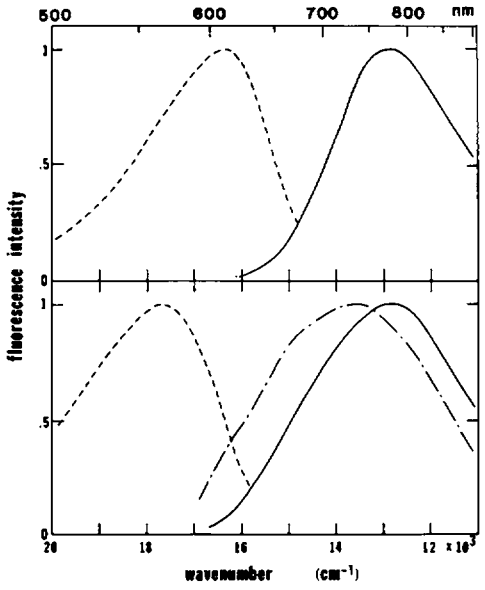

FIGURE 6 Fluorescence excitation (broken lines) and emission (solid lines) spectra of the purple membranes suspended at pH 7.0 (*lower* panel) and at pH 2.6 (*upper*). The chain line in the lower panel shows the emission spectrum observed at highly acidic pH (−0.5). The vertical scale is expressed in the unit of quanta per wavenumber.

of a linear polyene [Hudson and Kohler, 1973]. For the retinylidene chromophore with the protonated Schiff base, recent theoretical studies have suggested that the energy level of the allowed excited state ($^1B_u^+$) is far below the other excited singlet states (Birge, 1981). It appears that the emission originates from the first allowed excited state, irrespective of pH.

It has been shown by Mathies and Stryer (1976) that exictation of retinal to the first allowed excited state ($^1B_u^+$) is accompanied by a large change in the magnitude of the permanent dipole moment (or shift of a net positive charge toward the ionone ring). This change can cause a charge to displace near the retinylidene moiety, as long as a mobile charge exists. It is likely that the large Stokes shift observed at neutral pH is caused by a charge displacement induced immediately after excitation. At acidic pH, most of the negative charges in the protein are neutralized so that a significant charge displacement (or a large Stokes shift) may no longer be induced.

Excited State Dynamics of Bacteriorhodopsin

We found that the fluorescence intensity is almost independent of temperature at >0°C (Fig. 7), whereas Shapiro et al. (1978) observed a curious temperature dependence of the quantum yield of bacteriorhodopsin emission at lower temperatures. Their data (the closed circles in Fig. 7) shows a sharp temperature dependence, particularly obvious at <100 K. To explain both the temperature dependence and the pH dependence of the emission kinetics, we propose a model of the excited-state dynamics of bacteriorhodopin, as shown in Fig. 8. The model involves the following assumptions.

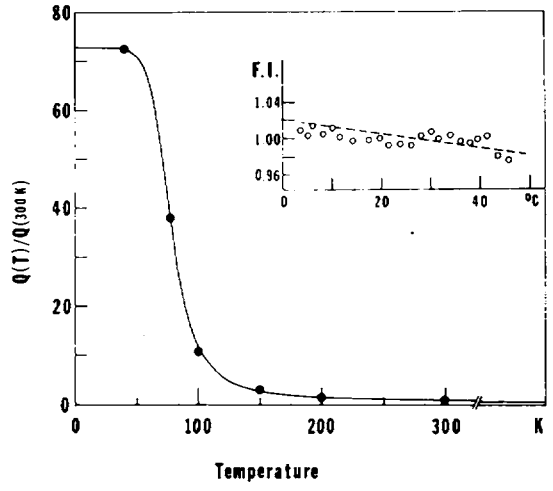

FIGURE 7 Temperature dependence of the fluorescence intensity (*F.I.*) observed above 740 nm after excitation at 540 nm of the dark-adapted purple membrane (open circles) (data from this paper). Temperature dependence of the quantum yield $Q(T)$ of bacteriorhodopsin emission reported by Shapiro et al. (1978) (closed circles). Solid and broken lines are the theoretical curves that were calculated using the parameters $Q(0) = 73 \times Q(300\text{ K})$, $Q(\infty) = 0.76 \times Q(300\text{ K})$, $T_c = 78$ K, and $\theta = 600$ K. In derivation of the broken line, it was assumed in Eq. B5 that $f_I(>740\text{ nm})/f_{II}(>740\text{ nm}) = 0.5$.

(*a*) At neutral pH, proton transfer to a base B_I^- (from a protonated residue, B_2H) occurs immediately after excitation:

$$bR_I(trans) \rightarrow bR_I^*(trans) \rightarrow bR_{II}^*(trans),$$

where bR_I represents bacteriorhodopsin with the negatively charged base B_I^-, which is protonated in bR_{II}; the residue B_2H is deprotonated in bR_{II}; and the asterisks (*) on the bRs denote the radiative states.

(*b*) The transition from bR_I^* to bR_{II}^* can occur via two processes; a thermally-activated process and a quantum-mechanically allowed process (tunneling process). The rate k_{cd}^{th} of the thermal process can be expressed by an Arrhenius-type function: $k_{cd}^{th} = \exp(-\theta/T)$, where T is the absolute temperature. The rate k_{cd}^{qm} of the other process is temperature independent. As soon as the state bR_{II}^* appears, the chromophore is deactivated. The deactivation rate k_i^{II} is very large (~1 ps^{-1}), irrespective of temperature. Such a transition may be possible if the conformation of the chromophore is strongly perturbed by the ionized residue B_2^-. In the acidic form bR_{605}^{acid}, the residues B_1H and B_2H are always protonated and the radiative state decays much more slowly.

Some of the assumptions in the above model have been already suggested by other workers: the idea of proton transfer has been proposed by Lewis (1978) and by Mathies and Stryer (1976) and the idea of the tunneling process was hinted by the observation of the deuterium isotope effect on the primary photochemical events of bacteriorhodopsin (Applebury et al., 1978).

Owing to assumption *b*, the fluorescence quantum yield can be approximated by the following function of temperature. (Its derivation is given in Appendix B):

$$Q(T) = Q(\infty) + [Q(0) - Q(\infty)]/[1 + \exp(\theta/T_c - \theta/T)],$$

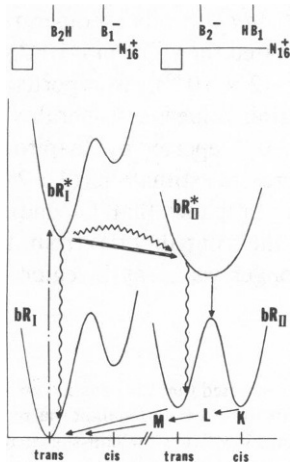

FIGURE 8 A model of the excited state dynamics of bacteriorhodopsin.

where $Q(0)$ and $Q(\infty)$ are the fluorescence quantum yields that would be observed at the two extreme temperatures; T_c is a constant with a dimension of temperature; and θ multiplied with a Boltzmann constant k_B represents the activation energy of the proton transfer via the thermal process. (The first and second terms in the above equation represent the quantum yields of emission from bR_{II}^* and from bR_I^*, respectively.) The solid curve in Fig. 7 represents the fluorescence quantum yield that was predicted from this equation, in which the following values of the parameters were assumed; T_c = 78 K, $Q(0)/Q(300\ K)$ = 73, $Q(\infty)/Q(300\ K)$ = 0.76, and θ = 600 K. The fluorescence intensity (above 740 nm) that would be predicted using the same values of the parameters (and Eq. B5) is shown by the broken line in Fig. 7. There is excellent coincidence between the theoretical curves and the experimental data, suggesting that the present model explains at least some essential parts of the primary photochemical events of bacteriorhodopsin.

At room temperature, emission from bR_{II}^* is calculated to be ~3 times as intense as emission from bR_I^*. At low temperatures, emission from bR_I^* is expected to become dominant; ~150 K, its emission is expected to be as intense as emission from the other emitting state (bR_{II}^*). This dependence agrees with previous reports that a sharp temperature dependence of the emission spectrum profile occurs at 100–150 K, below which the Stokes shift becomes smaller. At nitrogen temperature, the gap between the absorption peak (at 580 nm) and the emission peak (at 720 nm) is ~3,500 cm^{-1} (Lewis et al., 1976; Shapiro et al., 1978).

Fluorescence Quantum Yield and Lifetime

The question arises as to whether or not the emitting species (at neutral pH) is identical to the excited state from which the K_{590} intermediate originates. To answer this question, we need to compare the experimentally observed fluorescence lifetime with the lifetime calculated from the fluorescence quantum yield. With respect to the fluorescence quantum yield Q (at room temperature), Lewis et al. (1976) first estimated the value of $\sim 10^{-4}$, whereas a much smaller value ($Q \sim 2 \times 10^{-5}$) was reported by Govindjee et al. (1978). The latter value is considerably smaller than the value of $1–2.5 \times 10^{-4}$ reported by Shapiro et al. (1978) and the value of the present estimation ($Q = 2.5–2.7 \times 10^{-4}$ for bR^{trans}). It seems probable that Govindjee et al. (1978) underestimated the contribution from the fluorescence emitted in the longer wavelength region (e.g., above 700 nm; see Fig. 9).[1]

[1]Kriebel et al. (1979) reported that the emission peak shifted from 735 to 715 nm as the intensity of the excitation light was reduced from 3 W/cm^2 to 50 $\mu W/cm^2$. To check whether the emission that we observed comes from bR or from some photoproduct (e.g., a pseudo-bR proposed by Kriebel et al., 1979), we changed the intensity of the excitation light in the range between 10^{-7} and 10^{-3} W/cm^2 and collected fluorescence passing through various optical filters (Fuji-Film SC-66 or -74). We then found that the ratio of the fluorescence intensity above 740 nm to the intensity above 660 nm was always 0.55, independent of the intensity of the excitation light. This result allowed us to conclude that our spectrum shown in Fig. 9 represents the emission spectrum of bR. Because the sensitivity of the photomultiplier tube used decreases monotonously but slowly with increasing wavelength, the above result indicates that the center of the emission spectrum of bR should be around or above 740 nm, which is consistent with our spectrum in Fig. 9.

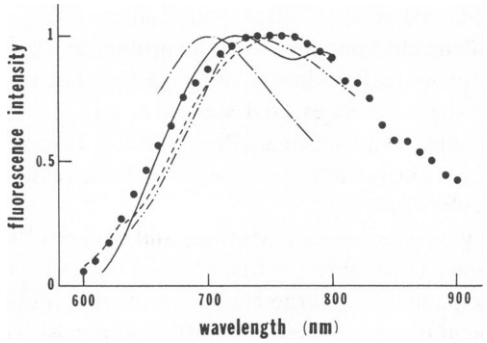

FIGURE 9 Comparison of the fluorescence emission spectra of bacteriorhodopsin (at neutral pH) reported from the various laboratories: (---) from Lewis et al. (1976); (— · · —) from Gillbro et al. (1977); (— · —) from Govindjee et al. (1978); (——) from Shapiro et al. (1978); and (●) from the present paper. The spectra measured at room temperature (or at 250 K for the data of Shapiro et al., 1978) are compared. The vertical scale is expressed in the unit of quanta per wavelength.

By using the present estimation and the radiative lifetime of ~6 ns (as calculated from the absorption spectrum), the fluorescence lifetime of ~2 ps was calculated for the case in which there were no branching process in the excited state (assuming a single-exponential fluorescence decay). This calculated value is close to the experimental lifetime (1.5–3 ps) inferred by Alfano et al. (1976) and by Shapiro et al. (1978), whereas a longer lifetime (15 ps) was reported by Hirsch et al. (1976). Although the data of Hirsch et al. (1976) seems to show the highest time resolution, we have noticed that their fluorescence decay curve can no longer be described with a single-exponential function. The decay constant of 15 ps seems to have been derived from an analysis of the tail portion of the decay curve. The moment-method analysis (Isenberg and Dyson, 1969) would give a shorter average lifetime ($\langle \tau_i^2 \rangle / \langle \tau_i \rangle$ = 6 ps), which means that the decay curve consisted of dominant components with decay constants $<<$6 ps and a minor component with the decay constant of 15 ps. Very recently, Sharkov et al. (1983) reported that the fluorescence lifetime is <2 ps.

The present model predicts a nonsingle-exponential fluorescence decay curve, especially at room temperature. The lifetime of bR_I^* is calculated to be ~0.4 ps and the lifetime of bR_{II}^* is expected to be 1–2 ps if the radiative lifetime is not affected by the charge displacement.

Because the emission spectra of bR_I^* and of bR_{II}^* are supposed to be different from each other, the fluorescence decay curve is expected to depend on the emission wavelength. Although this dependence has not been discussed in previous reports, it may explain the discrepancy among the values reported for the fluorescence lifetime at room temperature.

The present model can explain quantitatively the fluorescence lifetimes observed at various temperatures: $\tau = 40$ ps at 90 K (Alfano et al., 1976) and $\tau = 60 \pm 15$ ps at 77 K (Shapiro et al., 1978). Because at low temperature bacteriorhodopsin emission is expected to come mainly from the bR_I^*, the fluorescence decay curve can be approximated with a single-exponential decay, the decay constant of which is expressed as the following function of temperature

$$\tau(T) = \tau_0 Q(0)/[1 + \exp(\theta/T_c - \theta/T)],$$

where τ_0 is the radiative lifetime of the retinylidene chromophore whose value is expected to be ~6 ns from the absorption spectrum. When values of $Q(0) = Q(300\text{ K}) \times 73 = 0.02$ (± 0.002), $\theta = 600$ K, and $T_c = 78$ K are used, the fluorescence lifetime at 90 K and at 77 K are calculated to be 30 (± 4) ps and 60 (± 10) ps, respectively. Coincidence between the theoretical and experimental fluorescence lifetimes is good. It is likely that the main pathway of the *trans* photocycle involves the excited states bR_I^* and bR_{II}^*.

Primary Photochemical Reaction of Bacteriorhodopsin

In Fig. 8, we have supposed that $bR_{II}(cis)$ corresponds to the K_{590} intermediate. According to the above assignment, the photoreaction after excitation of K_{590} does not involve the excited state bR_I^*. Because bR_I is supposed to be the main emitting species at low temperature, the present model is consistent with the observation that K_{590} is much less fluorescent than bR_{570} at low temperature (Govindjee et al., 1978). It is also easy to explain the recent observation that the reverse reaction $K_{590} \rightarrow bR_{570}$ is much faster than the forward reaction (Kryukov et al., 1981).

An argument against the identification of the emitting species as a photochemically important excited state was proposed previously (Ottolenghi, 1980; Birge, 1981). Such an argument was based on the interpretation that, especially at low temperature, the rise time of the K_{590} state is shorter than the fluorescence lifetime. The rates reported for K_{590} formation are, for example, 10 ps at room temperature, 20 ps at 70 K, and 36 ps at 4 K (Applebury et al., 1978). However, it is important to notice that the quantum efficiency of formation of the emitting species is not small but rather close to 1, and therefore that its formation and decay processes should be accompanied by significant absorption changes. These corresponding changes are not seen in the data reported by Applebury et al.[2] It seems possible that the kinetics of the primary photoreaction depend on some parameters other than temperature (e.g., the intensity of excitation light). We feel that a simultaneous measurement of fluorescence and absorption kinetics is necessary for quantitative discussion.

APPENDIX A

Fluorescence Polarization in an Anisotropic System

Here we shall consider the polarization of fluorescence from the retinylidene chromophores in a stacked sample of the purple membranes. Generally, the polarization degree of fluorescence depends on the spatial arrangement of the optical components in a fluorometer as well as the orientational correlation between absorption and emission dipole moments of a fluorophore. When fluorophores (in the ground state) are isotropically oriented, the most convenient arrangement of optical components is obvious; i.e., it is usual to measure fluorescence emission at a right angle to the propagation direction of the excitation light beam (Eq. 3). When fluorophores are anisotropically oriented, the best arrangement depends on what kind of information must be extracted about the fluorophore. Our present interest is to obtain information about the orientation of the absorption and emission dipole moments of the retinylidene chromophore with reference to the purple membrane.

Fig. 10 shows a diagram of the optical system adopted in the present study. The main feature is as follows: A stacked sample of the purple membranes on a quartz plate (located in the x-y plane) is irradiated by a linearly polarized light beam propagating in a direction (in the x-z plane)

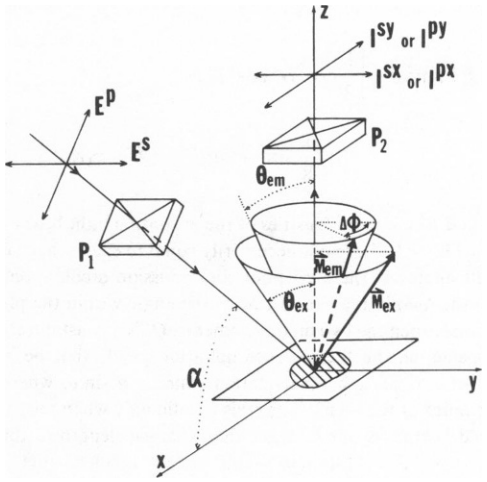

FIGURE 10 Optical arrangement for the measurement of the polarization degrees p^s and p^p of fluorescence from oriented purple membranes. P_1 and P_2 represent a polarizer and analyzer, respectively. M_{ex} and M_{em} denote the absorption and emission dipole moments, respectively.

[2]With weak excitation light pulses, Gillbro and Sundström (1983) have very recently observed absorption kinetics completely different from those reported previously. Although they introduced the idea of pseudo-bR to explain their data, we think that our model can explain their data well; the time constants of absorption recovery at 570 nm are 48 ps at 100 K and 62 ps at 77 K, which agree with the fluorescence lifetimes predicted by our model.

that makes an angle of α with x-axis. Fluorescence emission is viewed from a direction normal to the plate. Now, let us define the following polarization degrees of fluorescence:

$$p^s = (I^{sx} - I^{sy})/(I^{sx} + I^{sy}) \tag{A1}$$

$$p^p = (I^{px} - I^{py})/(I^{px} + I^{py}), \tag{A2}$$

where I^{sx} and I^{sy} (or I^{px} and I^{py}) are the principal components of polarized fluorescence that are observed when the polarization plane of the incident light beam is perpendicular (or parallel) to the plane of incidence.

The Simplest Case. We shall first consider the fluorescence polarizations p^s and p^p in such a system that (*a*) all of the purple membranes are stacked parallel to the plate, (*b*) the chromophores in the purple membrane are distributed with perfect C_3 symmetry and all of them have the same tilt angle with respect to the membrane normal, and (*c*) energy transfer between the neighboring chromophores is absent. Then the fluorescence intensities appearing in Eqs. A1 and A2 can be expressed as follows

$$I^{sx} = Q'E^s \sin^2\theta_{ex} \sin^2\theta_{em}\left(\frac{1}{2} + \frac{1}{4}\cos 2\Delta\phi\right) \tag{A3}$$

$$I^{sy} = Q'E^s \sin^2\theta_{ex} \sin^2\theta_{em}\left(\frac{1}{2} - \frac{1}{4}\cos 2\Delta\phi\right) \tag{A4}$$

$$I^{px} = Q'E^p \sin^2\theta_{em}\left[\frac{1}{2}\cos^2\alpha' \cos^2\theta_{ex} + \frac{1}{8}\sin^2\alpha' \sin^2\theta_{ex}(2 - \cos 2\Delta\phi)\right] \tag{A5}$$

$$I^{py} = Q'E^p \sin^2\theta_{em}\left[\frac{1}{2}\cos^2\alpha' \cos^2\theta_{ex} + \frac{1}{8}\sin^2\alpha' \sin^2\theta_{ex}(2 + \cos 2\Delta\phi)\right], \tag{A6}$$

where E^s and E^p are the intensities of the excitation light beam within the membrane (E^s and E^p are not necessarily equal to each other); θ_{ex} and θ_{em} are the tilt angles of the absorption and emission dipole moments with respect to the membrane normal; $\Delta\phi$ is the angle within the plane of the membrane between the two dipole moments; Q' is a constant, the value of which depends on the fluorescence quantum yield; and the angle α' is related to the angle α by the relation, $\sin\alpha = n \sin\alpha'$, where n is the refractive index of the membrane (this is valid only when the thickness of the stacked sample is much larger than the wavelength of the incident light; otherwise, the constant n should have a smaller value). Inserting Eqs. A3–A6 into Eqs. A1 and A2, we obtain

$$p^s = \frac{1}{2}\cos 2\Delta\phi \tag{A7}$$

$$p^p = -\frac{1}{2}\cos 2\Delta\phi \frac{\sin^2\alpha' \sin^2\theta_{ex}}{2\cos^2\alpha' \cos^2\theta_{ex} + \sin^2\alpha' \sin^2\theta_{ex}}. \tag{A8}$$

The last equation can be written as follows:

$$-\frac{1}{2}\left(\frac{p^s}{p^p} + 1\right)\tan^2\alpha' = \cot^2\theta_{ex}. \tag{A9}$$

Thus measurements of the polarization degrees p^s and p^p will allow us to determine the angle $\Delta\phi$ as well as the angle θ_{ex}.

Actual System. In the above derivation, we have not taken into account the possibilities of rotational motion of the chromophore in the membrane, of energy transfer between the neighboring chromophores, and so on. Now we shall consider their effect on the polarization degrees.

If the chromophore has a rotational mobility, Eq. A7 should be written as follows

$$p^s = \frac{\langle \sin^2\theta_{ex} \sin^2\theta_{em} \cos 2\Delta\phi\rangle}{\langle 2\sin^2\theta_{ex} \sin^2\theta_{em}\rangle}, \tag{A10}$$

where $\langle\ \rangle$ denotes the average of the possible orientation of the absorption and emission dipole moments.

If energy transfer occurs between the neighboring chromophores (existing in the same membrane), Eq. A7 should be rewritten as follows (Eq. A9 is unchanged):

$$p^s = \frac{1}{2}\left[1 - \frac{3}{2}(\eta + \eta')\right]\cos 2\Delta\phi + \frac{\sqrt{3}}{4}(\eta - \eta')\sin 2\Delta\phi, \tag{A11}$$

where the sum $\eta + \eta'$ is the probability that fluorescence emission comes from chromophores other than an initially excited chromophore (and those oriented parallel to it) and the term $\eta - \eta'$ is a result of the difference in the efficiency of energy transfer between two acceptors existing at the same distance from a donor (Kouyama et al., 1981).

Disorder in the stacking of the purple membranes will cause a slight modification in Eqs. A7 and A9:

$$p^s = \frac{1}{2}\cos 2\Delta\phi\,(1 - \langle\theta_m^2\rangle_m \cot^2\theta_{ex}) + 0(\langle\theta_m^2\rangle \cos\theta_{em}) \tag{A12}$$

$$-\frac{1}{2}\left(\frac{p^s}{p^p} + 1\right)\tan^2\alpha' = \cot^2\theta_{ex} \cdot \left[1 + \frac{1}{2}\langle\theta_m^2\rangle_m(\tan^2\theta_{ex} - 1 - 2\cot^2\theta_{ex}) + 0(\langle\theta_m^2\rangle_m \cos\theta_{em})\right], \tag{A13}$$

where θ_m is the tilt angle of the membrane with respect to the plate, and $\langle\ \rangle_m$ denotes the average of the possible orientations of the purple membranes in a stacked sample.

APPENDIX B

Emission Kinetics of Bacteriorhodopsin

We shall consider the emission kinetics of bacteriorhodopsin, assuming the main processes in the excited state can be described by the scheme as shown in Fig. 8. The time course of the probability of finding each excited state after excitation of one molecule of bacteriorhodopsin at time 0 is given by the following equations:

$$bR_I^*(t) = \exp(-\kappa_1 t) \tag{B1a}$$

$$bR_{II}^*(t) = k_{cd}[\exp(-\kappa_1 t) - \exp(-\kappa_2 t)]/(\kappa_2 - \kappa_1). \tag{B1b}$$

Here $\kappa_1 = k_f^I + k_{nr}^I + k_{cd}$ and $\kappa_2 = k_f^{II} + k_{nr}^{II}$; k_f and k_{nr} are the rate constants of radiative (fluorescence) and nonradiative processes to the corresponding ground states, respectively; and k_{cd} is the rate constant of the charge displacement (or the proton transfer; $k_{cd} = k_{cd}^{th} + k_{cd}^{qm}$, where k_{cd}^{th} and k_{cd}^{qm}, represent the rate constants of the thermally activated and the quantum mechanically allowed processes, respectively). The fluores-

cence intensity that would be observed at time t and at wavelength λ, $F(t;\lambda)$, is given by

$$F(t;\lambda) = k_f^{I} \cdot f_I(\lambda) \cdot bR_I^*(t) + k_f^{II} \cdot f_{II}(\lambda) \cdot bR_{II}^*(t), \quad (B2)$$

where $f_I(\lambda)$ and $f_{II}(\lambda)$ represent the profiles of the emission spectra from bR_I^* and from bR_{II}^*, respectively, and they satisfy the equation: $\int f_{I,II}(\lambda)d\lambda = 1$. Substitution of Eq. B1 into B2 gives the following equation

$$F(t;\lambda) = C_1(\lambda)\exp(-\kappa_1 t) + C_2(\lambda)\exp(-\kappa_2 t), \quad (B3)$$

where

$$C_1(\lambda) = k_f^{I} \cdot f_I(\lambda) + k_f^{II} \cdot k_{cd} \cdot f_{II}(\lambda)/(\kappa_2 - \kappa_1) \quad (B4a)$$

$$C_2 = -k_f^{I} \cdot k_{cd} \cdot f_{II}(\lambda)/(\kappa_2 - \kappa_1). \quad (B4b)$$

The fluorescence emission spectrum and quantum yield are given by

$$f(\lambda) = Q_I f_I(\lambda) + (k_{cd}/\kappa_1) Q_{II} f_{II}(\lambda) \quad (B5)$$

$$Q = Q_I + (k_{cd}/\kappa_1) Q_{II}, \quad (B6)$$

where

$$Q_I = k_f^{I}/\kappa_1 = k_f^{I}/(k_f^{I} + k_{nr}^{I} + k_{cd}^{qm} + k_{cd}^{th}) \quad (B7a)$$

$$Q_{II} = k_f^{II}/\kappa_2 = k_f^{II}/(k_{nr}^{II} + k_f^{II}). \quad (B7b)$$

When only the rate constant k_{cd}^{th} is dependent strongly on temperature and its temperature dependence can be expressed by an Arrhenius-type function [$\propto \exp(-\theta/T)$], Eq. B7a is reduced to

$$Q_I(T) = k_f^{I}/(k_f^{I} + k_{nr}^{I} + k_{cd}^{qm}) \cdot [1 + \exp(\theta/T_c - \theta/T)]. \quad (B8)$$

When the second term in Eq. B6 does not vary much with temperature, the fluorescence quantum yield Q can be approximated as follows

$$Q(T) = Q(\infty) + [Q(0) - Q(\infty)] / [1 + \exp(\theta/T_c - \theta/T)], \quad (B9)$$

where $Q(0)$ and $Q(\infty)$ are the quantum yields that would be observed at two extreme temperatures.

We are grateful to Drs. W. Stoeckenius, R. R. Birge, T. Kobayashi, R. A. Bogomolni, P. K. Wolber, Y. Kimura, and T. Furuno for their kind suggestions. We thank Mrs. Nakajima for her skillful assistance.

This work was supported by a research grant for Solar Energy Conversion Photosynthesis given by Japanese Science and Technology Agency and by grants-in-aid from the Ministry of Education, Science and Culture of Japan.

Received for publication 6 June 1983 and in final form 8 May 1984.

REFERENCES

Alfano, R. R., W. Yu, R. Govindjee, B. Becher, and T. G. Ebrey. 1976. Picosecond kinetics of the fluorescence from the chromophore of the purple membrane protein of *Halobacterium halobium*. *Biophys. J.* 16:541–545.

Applebury, M. L., K. S. Peters, and R. Rentzepis. 1978. Primary intermediates in the photochemical cycle of bacteriorhodopsin. *Biophys. J.* 23:375–382.

Berlman, I. B. 1971. Handbook of Fluorescence Spectra of Aromatic Molecules. Academic Press, Inc., New York. 473 pp.

Birge, R. R. 1981. Photophysics of light transduction in rhodopsin and bacteriorhodopsin. *Ann. Rev. Biophys. Bioeng.* 10:315–354.

Eastman, J. W. 1967. Quantitative spectrofluorimetry: the fluorescence quantum yield of quinine sulfate. *Photochem. Photobiol.* 6:55–72.

Fischer, U., and D. Oesterhelt. 1979. Chromophore equilibra in bacteriorhodopsin. *Biophys. J.* 28:211–230.

Gillbro, T., A. N. Kriebel, and U. P. Wild. 1977. On the origin of the red emission of light adapted purple membrane of *Halobacterium halobium*. *FEBS (Fed. Eur. Biochem. Soc.) Lett.* 78:57–60.

Gillbro, T., and V. Sundström. 1983. Picosecond kinetics and a model for the primary events of bacteriorhodopsin. *Photochem. Photobiol.* 37:445–455.

Govindjee, R., B. Becher, and T. G. Ebrey. 1978. The fluorescence from the chromophore of the purple membrane protein. *Biophys. J.* 22:67–77.

Henderson, R. 1975. The structure of the purple membrane from *Halobacterium halobium*. Analysis of the x-ray diffraction pattern. *J. Mol. Biol.* 93:123–138.

Hirsch, M. D., M. A. Marcus, A. Lewis, H. Mahr, and N. Frigo. 1976. A method for measuring picosecond phenomena in photolabile species. The emission lifetime of bacteriorhodopsin. *Biophys. J.* 16:1399–1409.

Hudson, B. S., and B. E. Kohler. 1973. Polyene spectroscopy: the lowest energy excited singlet state of diphenyloctatetrane and other linear polyenes. *J. Chem. Phys.* 59:4984–5002.

Ippen, E. P., C. V. Shank, A. Lewis, and M. A. Marcus. 1978. Subpicosecond spectroscopy of bacteriorhodopsin. *Science (Wash. DC).* 200:1279–1281.

Isenberg, I., and R. D. Dyson. 1969. The analysis of fluorescence decay by a method of moments. *Biophys. J.* 9:1337–1350.

Kaufmann, K. J., P. M. Rentzepis, W. Stoeckenius, and A. Lewis. 1976. Primary photochemical processes in bacteriorhodopsin. *Biochem. Biophys. Res. Commun.* 68:1109–1115.

Kinosita, K., Jr., R. Kataoka, Y. Kimura, O. Gotoh, and A. Ikegami. 1981. Dynamic structure of biological membranes as probed by 1,6-diphenyl-1,3,5-hexatriene: a nanosecond fluorescence depolarization study. *Biochemistry.* 20:4270–4277.

Kouyama, T., Y. Kimura, K. Kinosita, Jr., and A. Ikegami. 1981. Location and orientation of the chromophore in bacteriorhodopsin: analysis by fluorescence energy transfer. *J. Mol. Biol.* 153:337–359.

Kriebel, A. D., T. Gillbro, and U. P. Wild. 1979. A low temperature investigation of the intermediates of the photocycle of light-adapted bacteriorhodopsin: optical absorption and fluorescence measurements. *Biochim. Biophys. Acta.* 546:106–120.

Kryukov, P. G., Yu. A. Lazrev, Yu. A. Matveetz, E. L. Terpugov, L. N. Chekulaeva, and A. V. Sharkov. 1981. Picosecond spectroscopy of deuterated bacteriorhodopsin on the primary photochemical event. *Stud. Biophys.* 83:101–108.

Lewis, A. 1978. The molecular mechanism of excitation in visual transduction and bacteriorhodopsin. *Proc. Natl. Acad. Sci. USA.* 75:549–553.

Lewis, A., J. P. Spoonhower, and G. J. Perreault. 1976. Observation of light emission from a rhodopsin. *Nature (Lond.).* 260:675–678.

Mathies, R., and L. Stryer. 1976. Retinal has a highly dipolar vertically excited singlet state: implications for vision. *Proc. Natl. Acad. Sci. USA.* 73:2169–2173.

Mowery, P. C., R. H. Lozier, Q. Chae, Y.-W. Tseng, M. Taylor, and W. Stoeckenius. 1979. Effect of acid pH on the absorption spectra and photoreactions of bacteriorhodopsin. *Biochemistry.* 18:4100–4107.

Naito, T., Y. Kito, M. Kobayashi, K. Hiraki, and T. Hamanaka. 1981. Retinal-protein interactions in bacteriorhodopsin monomers, dispersed in the detergent L-1960. *Biochim. Biophys. Acta.* 637:457–463.

Oesterhelt, D., and W. Stoeckenius. 1974. Isolation of the cell membrane of *Halobacterium halobium* and its fractionation into red and purple membrane. *Methods Enzymol.* 31:667–678.

Oesterhelt, D., M. Meentzen, and L. Schuhmann. 1973. Reversible dissociation of the purple complex in bacteriorhodopsin and identification of 13-*cis* and all-*trans* retinal as its chromophores. *Eur. J. Biochem.* 40:453–463.

Ottolenghi, M. 1980. The photochemistry of rhodopsin. *Advan. Photochem.* 12:97–200.

Shapiro, S. L., A. J. Campillo, A. Lewis, G. J. Perreault, J. P. Spoonhower, R. K. Clayton, and W. Stoeckenius. 1978. Picosecond and steady state, variable intensity and variable temperature emission spectroscopy of bacteriorhodopsin. *Biophys. J.* 23:383–393.

Sharkov, A. V., Yu. A. Matveetz, S. V. Chekalin, A. V. Konyashchenko, O. M. Brekhov, and B. Yu. Rootskov. 1983. Fluorescence of bacteriorhodopsin under subpicosecond light excitation. *Photochem. Photobiol.* 38:108–111.

Sperling, W., P. Carl, C. N. Rafferty, and N. A. Dencher. 1977. Photochemistry and dark equilibrium or retinal isomers and bacteriorhodopsin isomers. *Biophys. Struct. Mech.* 3:79–94.

Stoeckenius, W., R. H. Lozier, and R. Bogomolni. 1979. Bacteriorhodopsin and the purple membrane of *halobacteria. Biochim. Biophys. Acta.* 505:215–278.

Wahl, P. 1979. Time-resolved fluorometry. *In* Biochemical Fluorescence: Concepts. R. F. Chen, and H. Edelhoch, editors. Marcel Dekker Inc., New York. 1–41.

Weber, G., and F. W. J. Teale. 1957. Determination of the absolute quantum yield of fluorescent solutions. *Trans. Faraday Soc.* 53:646–655.